FOURTH EUROPEAN ROTORCRAFT AND POWERED LIFT AIRCRAFT FORUM

Paper No. 24

APPLICATION OF THE FINITE ELEMENT METHOD TO ROTARY-WING AEROELASTICITY

P. Friedmann and F. Straub
Mechanics and Structures Department
University of California at Los Angeles
Los Angeles, California, 90024, U.S.A.

September 13-15, 1978

Stresa – Italy

Associazione Italiana di Aeronautica ed Astronautica

Associazione Industrie Aerospaziali

APPLICATION OF THE FINITE ELEMENT METHOD TO ROTARY-WING AEROELASTICITY

P. Friedmann, Associate Professor

and

F. Straub, Graduate Student

Mechanics and Structures Department

University of California at Los Angeles

Los Angeles, California, 90024, U.S.A.

ABSTRACT

Recent research in rotary-wing aeroelasticity has indicated that all fundamental problems in this area are inherently nonlinear. The nonlinearities in this problem are due to the inclusion of finite slopes, due to moderate deflections, in the structural, inertia and aerodynamic operators associated with this aeroelastic problem. In this paper the equations of motion, which are both time and space dependent, for the aeroelastic problem are first formulated in P.D.E. form. Next the equations are linearized about a suitable equilibrium position. The spatial dependence in these equations is discretized using a local Galerkin method of weighted residuals resulting in a finite element formulation of the aeroelastic problem. As an illustration the method if applied to the coupled flap-lag problem of a helicopter rotor blade in hover. Comparison of the solutions with previously published solutions establishes the convergence properties of the method. It is concluded that this formulation is a practical tool for solving rotary-wing aeroelastic stability or response problems.

Introduction

Recent research[1] in rotary-wing aeroelasticity in general and hingeless rotor blades in particular, has established the inherently nonlinear nature of the rotary-wing aeroelastic stability problem. As a consequence, the correct treatment of this aeroelastic stability problem requires the derivation of the dynamic equations of equilibrium in a careful and consistent manner such that moderate deflections based upon the assumption of small strains and finite slopes are properly incorporated in the mathematical model[1,2]. When the equations of motion are formulated in this manner, nonlinear terms can appear in the structural, inertia and aerodynamic operators associated with this aeroelastic problem and the final equations of motion will have a partial differential nonlinear form[1,2].

This work was supported by the Structures Laboratory AVRADCOM Research and Technology Laboratories and NASA Langley Research Center, Hampton, Virginia under NASA NGR 05-007-414.

In rotary wing aeroelasticity the nonlinear equations of motion in partial differential form are usually solved by applying Galerkin's method to eliminate the spatial dependence of the problem[1-3]. This procedure yields a set of coupled nonlinear ordinary differential equations for the dynamics of the blade. It is common practice[1-3] to obtain actual aeroelastic stability boundaries by linearizing the equations of motion about an appropriate equilibrium position and extracting stability information from the eigendate associated with the linearized system.

Typical studies[1-3] dealing with practical blade configurations in hover or in forward flight are representative of the algebraic complexity encountered when applying Galerkin's method to rotary wing aeroelastic problems. From the inspection of these and similar studies it is clear that methods of solution based upon the modal Galerkin method lead to extremely cumbersome algebraic manipulations, which have to be carried out manually or by alternative means such as algebraic manipulative systems. In some cases the amount of algebraic manipulations associated with the global Galerkin method is so excessive as to prohibit treatment of complicated blade configuration in a realistic manner. Therefore in this paper the spatial dependence will be eliminated using a Galerkin type finite element method. This essentially local Galerkin method enables one to discretize the partial differential equations of motion directly. Consequently a significant reduction in the algebraic manipulative labour required for the solution of the problem is accomplished.

During the past fifteen years the finite element method has undergone explosive growth and at the present it has evolved from a structural analysis tool to a general mathematical method for solving partial differential equations, which is competitive with finite differences, for general applications, and superior to finite differences in structural dynamic applications[4-7]. For conservative self adjoint, linear problems the finite element model for the system can be conveniently generated by applying appropriate variational principles. Existence of these variational principles will also in most cases guarantee the convergence of the method. For nonself adjoint,nonconservative problems, such as the flutter or aeroelastic problem, variational principles are not available. Thus generation of the finite element model for aeroelastic, nonconservative systems is more complicated and convergence of the method is not quaranteed[8].

The rotary-wing aeroelastic problem is nonself adjoint, nonconservative and nonlinear, thus formulation of a finite element method for this problem is by no means straightforward. However finite element discretization of these equations of motion will essentially eliminate the cumbersome algebraic manipulations associated with the global Galerkin method.

The purpose of the present paper is to develop a <u>local</u> Galerkin method of weighted residuals[5-7,9,10] which is used to discretize the spatial dependence of the equations resulting in a finite element formulation of the rotary wing aeroelastic problem. This method is applied directly to the equations of motion in partial differential form and leads to a finite element formulation of the rotary-wing aeroelastic problem and avoids the excessive algebraic manipulations required by the application of Galerkin's method when using global modes (i.e. conventional method).

To illustrate the method and establish its convergence properties the method is applied to some typical rotating blade free vibration problems

and to the coupled flap-lag aeroelastic stability calculation of a helicopter rotor blade in hover. Comparison of the solutions obtained, by using the finite element method, with previously published results is used to establish the convergence properties of the method. It is concluded that this formulation has the potential of becoming a powerful and practical tool for solving rotary wing aeroelastic stability or response problems.

Finally, it is worthwhile mentioning that for the case of rotating blade vibration problems in both linear and nonlinear formulations[11-13] the integrating matrix method has been successfully used to eliminate the spatial dependence in the problem. White[14] has also used the integrating matrix method for the flap-pitch flutter calculation of a rotor blade in hover. The main advantage in using a Galerkin type finite element approach consists mainly of the considerable amount of research done by applied methematicians and engineers on establishing the numerical properties of this method. This vigorous ongoing research activity provides the aeroelastician with more information on the numerical aspects and particularly convergence properties of the method than is available on the integrating matrix method, which is narrower in its scope.

2. Brief Description of the Coupled Flap-Lag Equations of Motion

The coupled flap-lag equations of motion used in this study serve mainly as an illustrative example for the application of a Galerkin type finite element method to rotary-wing aeroelasticity. The flap-lag equations for hover are obtained from the general equations which have been presented in Reference 2, by an appropriate elimination of the terms associated with forward flight and the torsional degree of freedom.

The geometry of the problem is shown in Figures 1A and 1B. A few important assumptions made in the derivation of these equations are briefly stated below:

(1) The blade is assumed to have moderate deflections, which implies small strains and finite rotations or slopes. These elastic rotations are assumed to be of order ε_D($\varepsilon_D \cong 0.20$) so that terms of $0(\varepsilon_D)^2$ are negligible compared to terms of order one, 0. (1) The blade can bend in two mutually perpendicular directions. Initially the blade is straight, during deformation the Euler-Bernoulli assumption is used. The structural operators resulting from these assumptions have been presented in Reference 15, (2) The blade has only precone β_p, it is cantilevered to the hub and there is no built-in twist, (3) There is no coupling between blade and fuselage dynamics, (4) Two dimensional quasisteady aerodynamic loads are used, apparent mass, stall and compressibility are neglected, (5) An ordering scheme identical to the one used in Reference 2 is used and quantities having the magnitude of the squares of the blade slopes are neglected when compared to one, i.e.

$$0(1) + 0(\varepsilon_D^2) \cong 0(1)$$

Using these assumptions the coupled flap-lag equations of motion for hover can be written down as follows.

Axial equilibrium:

$$\bar{T}_{,x} + (\bar{x}_0 + \bar{e}_1) + 2\dot{\bar{v}} = 0 \qquad (1)$$

Flap equilibrium:

$$-B_{23}\,\bar{v}_{,xxxx} - B_{33}\,\bar{w}_{,xxxx} + (\bar{w}_{,x}\,\bar{T})_{,x} - \beta_p(\bar{x}_0 + \bar{e}_1) - 2\beta_p\dot{\bar{v}}$$

$$-\ddot{\bar{w}} + \Gamma\{\theta\,\bar{x}_0(\bar{x}_0 + 2\,\bar{e}_1) - (\bar{x}_0 + \bar{e}_1)\,\frac{R}{\ell}\,\lambda - \bar{x}_0\,\beta_p\bar{v} + (2\theta\,\bar{x}_0 - \frac{R}{\ell}\,\lambda)\dot{\bar{v}}$$

$$-(\bar{x}_0 + \bar{e}_1)\dot{\bar{w}} - \bar{x}_0\,\bar{v}\,\bar{w} + \bar{x}_0^{\,2}\,\bar{v}_{,x}\,\bar{w}_{,x} - \dot{\bar{v}}\,\dot{\bar{w}}\} = 0 \qquad (2)$$

Lag equilibrium

$$-B_{22}\,v_{,xxxx} - B_{23}\bar{w}_{,xxxx} + (\bar{v}_{,x}\bar{T})_{,x} + \frac{d}{d\psi}\int_0^{\bar{x}_0}(\bar{v}_{,x}^{\,2} + \bar{w}_{,x}^{\,2})\,d\bar{x}_0$$

$$+ \bar{v} - \ddot{\bar{v}} + 2\beta_p\dot{\bar{w}} + \Gamma\{\theta(\bar{x}_0 + \bar{e}_1)\,\frac{R}{\ell}\,\lambda + (\frac{R}{\ell}\,\lambda)^2$$

$$- \frac{C_{d0}}{a}\,\bar{x}_o(\bar{x}_0 + 2\bar{e}_1) + (2\,\frac{R}{\ell}\,\lambda\,\beta_p - \theta\,\bar{x}_0\,\beta_p)\bar{v} - (\theta\,\frac{R}{\ell}\,\lambda + 2\,\frac{C_{d0}}{a}\,\bar{x}_o)\dot{\bar{v}}$$

$$+ [2\,\frac{R}{\ell}\,\lambda - \theta(\bar{x}_o + \bar{e}_1)]\dot{\bar{w}} + (2\,\frac{R}{\ell}\,\lambda - \theta\,\bar{x}_0)\bar{v}\,\bar{w}_{,x}$$

$$- \frac{R}{\ell}\,\lambda\,\bar{x}_0\,v_{,x}\,w_{,x} + 2\beta_p\,\bar{v}\,\dot{\bar{w}} - \theta\,\dot{\bar{v}}\,\dot{\bar{w}} + \dot{\bar{w}}^2$$

$$+ 2\bar{v}\,\bar{w}_{,x}\,\dot{\bar{w}} - \bar{x}_0\,\bar{v}_{,x}\,\bar{w}_{,x}\,\dot{\bar{w}}\} = 0 \qquad (3)$$

The notation used in these equations is defined in Appendix A.

The boundary conditions are given by [2,15]

$$\text{at } \bar{x}_0 = 0 \qquad \bar{v} = \bar{w} = \bar{v}_{,x} = \bar{w}_{,x} = 0 \qquad (4)$$

$$\text{at } \bar{x}_0 = 1 \qquad \bar{T} = 0 \text{ and}$$

$$B_{22}\,\bar{v}_{,xxx} + B_{23}\,\bar{w}_{,xxx} = 0$$

$$B_{23}\,\bar{v}_{,xxx} + B_{33}\,\bar{w}_{,xxx} = 0$$

$$B_{22}\,\bar{v}_{,xx} + B_{23}\,\bar{w}_{,xx} = 0 \qquad (5)$$

$$B_{23}\,v_{,xx} + B_{33}\,w_{,xx} = 0$$

3. Implementation of Galerkin Type Finite Element Method

3.1 General Description of the Method

The local Galerkin method, resulting in a finite element discretization can be best clarified by illustrating its application to a simple system. Consider the following simple differential equation

$$R(q) + P(q) = F \tag{6}$$

which is defined in some domain D, such that R is a symmetric operator and P is a general operator, both operating on an unknown function q to yield a given function F. Furthermore the function q has to satisfy certain boundary conditions on the boundary S of the domain D.

Next, an approximate global solution having the form

$$q^g = \sum_{m=1}^{M} \Phi_m \, b_m \tag{7}$$

is assumed. Where Φ_m are linearly independent shape functions and b_m are undetermined parameters for this problem, q^g has to satisfy only the geometric boundary conditions.

The extended Galerkin method requires that the sum of the weighted residuals of both the differential equation and the natural boundary condition be zero[9], i.e.,

$$\int_D \Phi_m \, \varepsilon dD + \Phi_m \, \varepsilon_B|_S = 0 \tag{8}$$

$$\text{for } m = 1,2,\ldots M.$$

where

$$\varepsilon = R(q^g) + P(q^g) - F \tag{9}$$

and ε_B is the residual associated with the natural boundary conditions.

Integration by parts, applied on Eq. (8), reduces the order of differentiation in the symmetric operator R thus lowering the continuity requirements on the shape functions Φ_m, furthermore this algebraic step also yields terms, which cancel the contribution of the boundary residual in Eq. (8)

When formulating a finite element version of Galerkin's method the domain D is subdivided into E subdomains Ω^e, which are called elements. In each element an approximate solution of the form

$$q^e = \sum_{n=1}^{N} \psi_n^e \, a_n^e \tag{10}$$

is assumed. Where a_n^e are the nodal parameters and ψ_n^e are linearly independent shape functions defined only in the subdomain associated with the element Ω^e. This local approximation can be extended over the whole domain D by defining

$$\zeta_n^e = \begin{cases} \psi_n^e & \text{within } \Omega^e \\ 0 & \text{outside } \Omega^e \end{cases} \tag{11}$$

Using Eq. (11) the global approximation can be expressed as

$$q^g = \sum_{e=1}^{E} \sum_{n=1}^{N} \zeta_n^e \, a_n^e \tag{12}$$

After imposing compatibility conditions on the nodal parameters of adjacent elements (this is done during the process of assembly) equations (7) and (12) are equivalent.

Equation (8) can be rewritten using Eq. (12) as

$$\sum_{i=1}^{E} \sum_{n=1}^{N} \int_D \{[\bar{R}(\zeta_j^e, \zeta_n^i) + \zeta_j^e P(\zeta_n^i)] a_n^i - \zeta_j^e F\} = 0 \tag{13}$$

$$j = 1,2,\ldots N, \; e = 1,\ldots E$$

where $\bar{R}$ is obtained from R by means of the previously mentioned integration by parts. Equation (13) represents all weighted residuals for one element and for the total assemblage of elements (i.e. N*E weighted residuals), it represents an intermediate step and in reality only Eq. (14) is used.

As a consequence of the linear independence of the ζ_n^e functions, equation (13) can be also rewritten on the element level.

$$\sum_{n=1}^{N} \int_{\Omega_e} \{[\bar{R}(\psi_j^e, \psi_n^e) + \psi_j^e P(\psi_n^e)] a_n^e - \psi_j^e F\} = 0 \tag{14}$$

$$j = 1,2,\ldots N; \; e = 1,2,\ldots,E$$

Equation (14) thus represents a set of N equations for each element, from which the element matrices can be calculated.

3.2 Application to the Flap-Lag Problem in Hover

The flap-lag equations in hover were described in Section 2. To facilitate manipulation of these equations they are rewritten in matrix operator form

$$\begin{aligned} &[I]\{\ddot{q}\} - [C_{Ax}(\underset{\sim}{q}, \bar{x}_0)]\{\dot{q}\} + ([G] + [D_1(\bar{x}_0)] - \\ &-[D_2(\underset{\sim}{q}, \underset{\sim}{\dot{q}})] + [D_3(q, x_0)])\{\dot{q}\} - [C_{T2}(\underset{\sim}{q}, x_0)]\{\dot{q}\} \\ &+ ([S_B] - [S_{T1}(\bar{x}_0)] - [K_{ROT}] + [A_1(x_0)] + [A_2(\underset{\sim}{q}, \bar{x}_0)]\{q\} = \{F(x_0)\} \end{aligned} \tag{15}$$

where $\{q\} = \begin{Bmatrix} \bar{v} \\ \underset{\sim}{\bar{w}} \end{Bmatrix}$. Other quantities are defined in Appendix B. It should be noted that the tension $\bar{T}$ was eliminated using the axial equation.

According to Eq. (7), a global solution is given by

$$\{q^g\} = \sum_{m=1}^{M} [\Phi_m]\{b_m\} = [\Phi]\{b\} \tag{16}$$

Upon substitution into the differential equations and boundary conditions it yields the residuals $\{\varepsilon\}$ and $\{\varepsilon_B\}$. The weighted Galerkin residuals become

$$\int_0^1 [\Phi_m]^T \{\underset{\sim}{\varepsilon} + \underset{\sim}{\varepsilon}_p - \underset{\sim}{F}\}d\bar{x}_0 + [\Phi_m]^T \underset{\sim}{\varepsilon}_B\Big|_1 = 0 \tag{17}$$

$$m = 1,2,\ldots M$$

where

$$\underset{\sim}{\varepsilon}_R = [S_B]\{q^g\} - [S_{T1}]\{q^g\} - [C_{T2}]\{\dot{q}^g\}$$

$$= [B]\, D_x^{\,4}\{q^g\} - D_x([T_1]\{q^g\}) - D_x([T_2]\{\dot{q}^g\})$$

$$\underset{\sim}{\varepsilon}_B = -[B]D_x^{\,3}\{q^g\} + [B]D_x^{\,2}\{q^g\} + ([T_1] + [T_2])D_x\{q^g\}\Big|_{\bar{x}_0=1}$$

$$\underset{\sim}{\varepsilon}_p = [I]\{\ddot{q}^g\} + [C_{Ax}]\{\dot{q}^g\} + ([G] + [D_1] + [D_2] + [D_3])\{\dot{q}^g\}$$

$$+ (-[K_{ROT}] + [A_1] + [A_2])\{q^g\} \tag{18}$$

and $$D_x^{\,i} = \frac{d^i}{d\bar{x}_0^{\,i}}$$

Integrating by parts the $\underset{\sim}{\varepsilon}_R$ term, Eq. (17) becomes

$$\int_0^1 \{\underset{\sim}{\bar{\varepsilon}}_R + [\Phi_m]^T(\underset{\sim}{\varepsilon}_p - \underset{\sim}{F})\}d\bar{x}_0 = \underset{\sim}{0} \qquad m = 1,2,\ldots M \tag{19}$$

where

$$\underset{\sim}{\bar{\varepsilon}}_R = D_x^{\,2}[\Phi_m]^T[B]D_x^{\,2}\{q^g\} + D_x\,[\Phi_m]^T[T_1]\{q^g\} + D_x\,[\Phi_m]^T[T_2]\{\dot{q}^g\} \tag{20}$$

Inside the element the displacements are given by

$$\{q^e\} = \begin{Bmatrix} \bar{v}^e \\ \bar{w}^e \end{Bmatrix} = \sum_{n=1}^{N} \begin{bmatrix} \gamma_n & 0 \\ 0 & \eta_n \end{bmatrix} \begin{Bmatrix} h_n^{\,e} \\ g_n^{\,e} \end{Bmatrix}$$

$$= \begin{bmatrix} \underset{\sim}{\gamma}^T & \underset{\sim}{0} \\ \underset{\sim}{0} & \underset{\sim}{\eta}^T \end{bmatrix} \begin{Bmatrix} \underset{\sim}{h}^e \\ \underset{\sim}{g}^e \end{Bmatrix} = [\Psi(x_e)]\{a^e(\psi)\} \tag{21}$$

In the present analysis ordinary beam type bending[5-7] representation was chosen for modeling the flap-lag motion, the geometry of the element is illustrated in Figure 1B, where q_F and q_L represent symbolically the four nodal degrees of freedom associated with flapwise and lagwise bending respectively. Thus N = 4, $\gamma_n = \eta_n$ are cubic interpolation polynomials[5-7] and h_n^e, g_n^e represent nodal displacements and slopes for lag (h_n^e) and flap (g_n^e) respectively. For convenience the superscript e is omitted from the shape function matrix [Ψ].

As has been indicated previously stability boundaries in rotary wing aeroelasticity can be obtained by linearizing the equations of motion about an appropriate equilibrium position. For the case of coupled flap-lag in hover the equilibrium position is taken as the static nonlinear equilibrium position and the dynamic equations of motion are perturbed about this equilibrium position, i.e.,

$$\{a^e(\psi)\} = \{a^{e0}\} + \{\Delta\, a^e(\psi)\} \tag{22}$$

Equation (21) is now extended in the sense of Eq. (11) and substituted, together with Eq. (22), into Eq. (19). This yields the nonlinear static equilibrium position

$$([B^e] + [T_1^e] - [K_{ROT}^e] + [A_1^e] + [A_2^e])\{a^{e0}\} = \{F^e\} \tag{23}$$

where it should be noted that $[A_2^e]$ also depends on $\{a^{e0}\}$ and thus Eq. (23) is nonlinear.

Similarly the linearized dynamic equilibrium equations are given by

$$\begin{aligned}
&[I^e]\{\Delta\ddot{a}^e\} + ([G^e] + [D_1^e] - [D_2^e] + [D_3^e])\{\Delta\dot{a}^e\} \\
&+ [T_2^e]\{\Delta\dot{a}^e\} + \sum_{i=e+1}^{E} [T_2^{ei}]\{\Delta\dot{a}^i\} - [C_{Ax}^e]\{\dot{a}^e\} \\
&- \sum_{i=1}^{e-1} [C_{Ax}^{ei}]\{\Delta\dot{a}^i\} + ([B^e] + [T_1^e] - [K_{ROT}^e] + [A_1^e] + \\
&+ [A_2^e])\{\Delta a^e\} = \{0\} \qquad e = 1,2,\ldots E
\end{aligned} \tag{24}$$

Equations (23) and (24) are equations written at the element level, thus $[B^e]$, $[I^e]$..., etc. represent element matrices. For the cubic shape functions which have been selected, six point Gaussian quadrature yields the exact element matrices. Evaluation of the constant term F^e and the linear terms $[B^e]$, $[T_1^e]$, $[K_{ROT}^e]$, $[A_1^e]$ in the static equilibrium equations, Eqs. (23), is straightforward. The quadratic term, $[A_2^{e0}]$ depends on the static equilibrium position itself. Since the nonlinear equilibrium position equations are solved by iteration, $[A_2^{e0}]$ can be evaluated using the value of a^{e0} from the previous iterative step. All the terms in the dynamic equation, Eq. (24) are linear. However the matrices $[D_2^e]$, $[D_3^e]$, $[T_2^e]$, $[T_2^{ei}]$, $[C_{Ax}^e]$, $[C_{Ax}^{ei}]$ and $[A_2^e]$ depend on the static equilibrium position, which is a known quantity after the static problem has been solved.

The assembly of the element matrices into the complete system matrices is similar to the conventional finite element method, when utilizing the direct stiffness approach[5-7]. It should be noted however, that bandedness of the velocity proportional matrix is destroyed due to terms of type

$$\sum_{i=e+1}^{E} [T^{ei}]\{\Delta\dot{a}^{i}\} \quad \text{and} \quad \sum_{i=1}^{e-1} [C_{Ax}^{ei}]\{\Delta\dot{a}^{i}\}$$

which are a consequence of the inner integrals over the global domain in the operators $[C_{T2}]$ and $[C_{Ax}]$.

The considerable number of unknowns, representing the nodal degrees of freedom, in the finite element formulation can be reduced when modal analysis is used. Thus

$$\{a^{0}\} = [\bar{\Phi}]\{q^{0}\}$$
$$\{\Delta a\} = [\bar{\Phi}]\{\Delta q\} \qquad (25)$$

where $[\bar{\Phi}]$ is the modal transformation matrix containing the first M uncoupled modes, representing the free vibration mode shapes of a rotating blade. These mode shapes are also determined using the finite element method when applied to the rotating beam free vibration problem. Since the free vibration equations are self-adjoint, the Galerkin finite element method is, for this case, identical to the conventional finite element method. Thus $\{q^{o}\}$ and $\{\Delta q\}$ are reduced vectors of generalized coordinates

$$\{q^{0}\} = \{h_1^{0}, h_2^{0} \ldots h_M^{0}, g_1^{0}, g_2^{0}, \ldots g_M^{0}\}$$

Clearly, modal analysis provides an effective reduction in the size of the eigenvalue problem required for the solution of the dynamic system equations. This is a considerable advantage since determination of stability boundaries requires repeated solutions of the eigenvalue problem. Furthermore due to this approach the bandedness of the finite element system matrices becomes irrelevant since the reduced system matrices are fully populated anyway. Finally it is important to realize that modal analysis facilitates the solution of the nonlinear static equilibrium equations. Since the reduced number of unknowns allows one to calculate the derivatives of the nonlinear terms explicitly and an efficient algorithm based on the Newton-Raphson approach can be used.

The final equations, after modal reduction, for static equilibrium are

$$[S_L]\{q^{0}\} + [S_{NL}(q^{0})]\{q^{0}\} = \{C\} \qquad (26)$$

and for dynamic equilibrium

$$[M]\{\Delta\ddot{q}\} + [D]\{\Delta q^{0}\} + [K]\{\Delta q\} = 0 \qquad (27)$$

4. Results and Discussion

4.1 Method of Solution and Data Used in the Computations

Solution of Eqs. (26) and (27) is accomplished in two stages. First the nonlinear equations for the static equilibrium position Eqs. (26) are solved using a Newton-Raphson iterative scheme. Next the dynamic equations, Eqs. (27), are first transformed into first order state variable form[1], resulting in a standard eigenvalue problem which can be easily solved using conventional methods, stability[1] is determined from the sign of the real part of the eigenvalue $\lambda_k = \zeta_k + i\omega_k$.

In calculating numerical results certain simplifying assumptions were made, since the objective of the paper is primarily to illustrate the application of the Galerkin type finite element to rotary-wing aeroelasticity.

These simplifying assumptions are listed below:

(a) Mass and stiffness distributions were assumed to be constant along the span of the blade

(b) Inflow ratio was assumed to be constant over the blade and equal to the inflow at 0.75 span, i.e.

$$\lambda = (a\sigma/16)[(1 + 24\theta/a\sigma)^{1/2} - 1] \tag{28}$$

(c) For all cases considered, structural damping was assumed to be zero and the following numerical values were used in the calculations

$$a = 2\pi \; ; \; (C_{d0/a}) = 0.01 \; ; \; \beta_p = 0.0$$

4.2 Results

In order to determine the convergence properties of the finite element method the free vibration problem of a rotating beam vibrating in and out of plane of rotation is considered first. The fundamental flap and lag, uncoupled frequencies, of a rotating beam were calculated using two methods:

(a) a global Galerkin method in which five nonrotating modes of a uniform beam are used to obtain the fundamental, uncoupled, flap and lag frequencies of a rotating beam and

(b) using the Galerkin finite element method of weighted residuals.

Comparison between the two sets of results showing the uncoupled rotating flap and lag frequencies $\bar{\omega}_{F1}$ and $\bar{\omega}_{L1}$ as a function of the nonrotating frequencies is shown in Fig. 2. The results for the fundamental frequencies are identical with three or six elements, indicating that good accuracy can be obtained with a few number of elements.

Comparison of the first and second mode obtained using both methods is presented in Figure 3 for the nonrotating case, and two different speeds of rotation. For this case eight elements were used because it was more

convenient to plot the results when slightly more elements were used. From numerical convergence point of view six elements would have been also adequate. From these results it is clear that excellent agreement between the global Galerkin and Galerkin finite element method is obtained for both frequencies and mode shapes.

For completeness it should be mentioned that solutions for the flapwise free vibrations of a pinned-free rotating beam using a Galerkin type finite element method have been presented by Nagaraj and Shanthakumar[16]. Their treatment however was not based on the extended Galerkin method, thus the interpolation functions selected had to satisfy all the boundary conditions, resulting in a flapwise bending element with four degrees of freedom at each node, compared to two degrees of freedom per node used in the present treatment.

Next the method is applied to a typical rotary-wing aeroelastic problem. The coupled flap-lag aeroelastic problem in hover[1,17] is a convenient and simple example which can be used to illustrate the Galerkin finite element method. The numerical accuracy of the method can be best seen by comparing a global Galerkin solution based on one uncoupled rotating elastic mode for each degree of freedom with a local Galerkin finite element solution in which the blade is represented by three finite elements and, where for consistence with the global method, one uncoupled elastic rotating mode is used for each degree of freedom to reduce the number of nodal degrees of freedom. The comparison between the two methods is presented in Table 1. For two separate collective pitch angles θ, all pertinent values associated with these cases were evaluated. The agreement between the two methods is excellent when considering that only three elements are used to represent the blade. Similar comparisons were made for a variety of other cases, the results are not presented since they would have been repetitive of the behaviour illustrated by Table 1. The cases presented in Table 1 were stable configurations because the elastic coupling parameter R_e was taken as $R_e = 1.0$.

Convergence properties of the Galerkin finite element method when applied to the aeroelastic problem are considered next. It is important to note that convergence of Galerkin type methods in aeroelasticity can be established only by numerical experimentation[18], in rotary-wing aeroelastic problems this is further complicated due to their nonlinear nature. Convergence of the method can be investigated, alternatively, by varying the number of elements while retaining a fixed number of modes in the modal reduction process or by changing the number of modes and maintaining a fixed number of elements.

Figure 4 illustrates the convergence of stability boundaries for three different values of the elastic coupling parameter when the number of elements is allowed to vary from three to six, while the number of modes used in the modal reduction process is maintained at one mode for each elastic degree of freedom. In all cases shown in the figure the unstable regions tend to decrease as the number of elements is increased. The results for $N = 5$ and $N = 6$ are almost identical indicating that 4 or 5 elements are sufficient to capture the bending dynamics of the blade.

Figure 5 illustrates the convergence of a typical stability boundary when the number of elements is maintained at four and the elastic modes used in the modal reduction process is allowed to vary. As indicated in the figure the difference between taking two modes for each degree of freedom and one mode is relatively small. It is interesting to note

that convergence trends seem to differ depending whether the blade is soft inplane or stiff inplane when $R_e = 0$.

Finally it should be noted that the Galerkin type finite element method as formulated in this paper can be applied without any significant modification to more complicated aeroelastic problems such as the coupled flap-lag-torsion problem[1], or to coupled rotor fuselage dynamics. In these cases it can significantly reduce the algebraic manipulations required when compared to a global Galerkin method. Obviously since spatial discretization is applied directly to the partial differential equations, algebraic manipulations decrease however more computer time is spent in calculations. Thus one can say that a considerable amount of algebraic work is done numerically instead of using symbolic manipulation. For the flap-lag case the computer times required to generate stability boundaries were quite small since only a few elements are needed in order to accurately capture the dynamics of the blade.

5. Conclusions

The main conclusions obtained in this study are summarized below:

(1) The Galerkin finite element method is a practical tool for formulating and solving rotary wing aeroelastic problems. It significantly reduces the algebraic manipulative labor when compared to the application of the global Galerkin method to similar problems.

(2) Four or five elements are sufficient to capture the bending dynamics of the blade. When torsion is included it is envisioned that six to eight elements will be adequate for capturing the coupled bending-torsional dynamics of the blade.

(3) Normal mode transformation combined with a Galerkin finite element formulation reduces significantly the number of nodal degrees of freedom and enables one to deal efficiently with complex problems.

References

1. Friedmann, P., "Recent Developments in Rotary-Wing Aeroelasticity," Journal of Aircraft, Vol. 14, No. 11, November 1977, pp. 1027-1041.

2. Shamie, J. and Friedmann, P., "Effect of Moderate Deflections on the Aeroelastic Stability of a Rotor Blade in Forward Flight," Forum Proceedings of the Third European Rotorcraft and Powered Lift Aircraft Forum, Paper No. 24, 1977.

3. Hodges, D.H. and Ormiston, R.A., "Stability of Elastic Bending and Torsion of Uniform Cantilever Rotor Blades in Hover with Variable Structural Coupling," NASA TND-8192, April 1976.

4. Strang, G. and Fix, G., An Analysis of the Finite Element Method, Prentice Hall, 1973.

5. Gallagher, R.H., Finite Element Analysis, Prentice Hall, 1975.

6. Huebner, K.H., The Finite Element Method for Engineers, John Wiley, 1975.

7. Segerlind, L.J., Applied Finite Element Analysis, John Wiley, 1976.

8. Kikuchi, F., "A Finite Element Method for Non-Self-Adjoint Problems," International Journal of Numerical Methods in Engineering, Vol. 6, pp. 39-54, 1973.

9. Finlayson, B.A. and Seriven, L.E., "The Method of Weighted Residuals - A Review," Applied Mechanics Reviews, Vol. 19, No. 9, September 1966, pp. 735-748.

10. Hutton, S.G. and Anderson, D.L., "Finite Element Method: A Galerkin Approach," Journal of Engineering Mechanics Division of ASCE, October 1971, pp. 1503-1520.

11. Hunter, W.F., "The Integrating Matrix Method for Determining the Natural Vibration Characteristics of Propeller Blades," NASA TN D-6064, December 1970.

12. White, W.F. and Malatino, R.E., "A Numerical Method for Determining the Natural Vibration Characteristics of Rotating Non-uniform Cantilever Blades," NASA TM X-72751, October 1975.

13. Kvaternik, R.G., White, W.F., and Kaza, K.R., "Nonlinear Flap-Lag-Axial Equations of a Rotating Beam with Arbitrary Precone Angle," AIAA Paper 78-491, Proceedings of AIAA/ASME 19th Structures, Structural Dynamics and Materials Conference, Bethesda, Maryland, April 1978, pp. 214-227.

14. White, W.F., "Effect of Compressibility on Three-Dimensional Helicopter Rotor Blade Flutter," Ph.D. Dissertation, Georgia Institute of Technology, School of Aerospace Engineering, March 1973.

15. Rosen, A. and Friedmann, P., "Nonlinear Equations of Equilibrium for Elastic Helicopter or Wind Turbine Blades Undergoing Moderate Deformation," University of California, Los Angeles, School of Engineering and Applied Science Report, UCLA-ENG-7718, January 1977. (Revised June 1977).

16. Nagaraj, V.T. and Shanthakumar, P., "Rotor Blade Vibrations by the Galerkin Finite Element Method," Journal of Sound and Vibration, Vol. 43, No. 3, pp. 575-577, 1975.

17. Ormiston, R.A. and Hodges, D.H., "Linear Flap-Lag Dynamics of Hingeless Helicopter Rotor Blades in Hover," Journal of the American Helicopter Society, Vol. 17, No. 2, April 1972, pp. 2-14.

18. Kornecki, A., "On Application of Galerkin's Method to Non-Self-Adjoint Problems," Technion-Israel Institute of Technology, Dept. of Agricultural Engineering, Report No. 101, August 1970.

Appendix A. List of Symbols

a = two dimensional lift curve slope.

a_n^e = element nodal parameters.

$\underset{\sim}{a}^e$ = element nodal displacement vector.

$\underset{\sim}{a}$ = system nodal displacement vector.

$[A_1], [A_2], [A_1^e], [A_2^e], [\bar{A}_2^e]$ = aerodynamic operators and stiffness matrices defined in Appendix B.

b = semichord.

b_m = modal parameters (generalized coordinates).

$\underset{\sim}{b}_m, \underset{\sim}{b}$ = vector of generalized coordinates.

$$B_{22} = \frac{E}{m\Omega^2 \ell^4} [I_2 - (I_2 - I_3)\sin^2 R_c\theta]$$

$$B_{23} = \frac{E}{m\Omega^2 \ell^4}[(I_2 - I_3)\tfrac{1}{2}\sin 2R_c\theta]$$

$$B_{33} = \frac{E}{m\Omega^2 \ell^4}[I_3 + (I_2 - I_3)\sin^2 R_c\theta]$$

$[B], [B^e]$ = bending stiffness operators and matrices defined in Appendix B.

$\{C\}$ = forcing vector in final static equations, Appendix B.

C_{do} = profile drag coefficient.

$[C_{Ax}], [C_{Ax}^e], [C_{ax}^{ei}]$ = operators and matrices due to axial shortening effect, defined in Appendix B.

$[C_{T2}]$ = tension operator defined in Appendix B.

$$D_x^i = \frac{\partial^i}{\partial \bar{x}_0^i}$$ = differential operator.

$[D_1], [D_2], [D_3], [D_1^e], [D_2^e], [D_3^3]$ = aerodynamic damping operators and matrices defined in Appendix B.

$[D]$ = equivalent damping matrix, Appendix B.

E = Young's modulus of elasticity, also number of finite elements.

F = known function.

$\underset{\sim}{F}, \underset{\sim}{F}^e$ = constant forcing terms, defined in Appendix B.

$\underset{\sim}{q}^e = \underset{\sim}{q}^c_n =$ = element flap displacements generalized coordinate, mth flap mode.

$[G], [G^e]$ = gyroscopic operator and matrix, Appendix B.

$\underset{\sim}{h}^e = \{h^e_n\}$ = element lag displacements.

I_2 = principal moment of inertia for lagwise bending.

I_3 = principal moment of inertia for flapwise bending.

$[I], [I^e]$ = inertia operator and matrix, Appendix B.

$[K_{ROT}], [K^e_{ROT}]$ = operator defined in Appendix B.

$[K]$ = stiffness matrix in final dynamic equations, see Appendix B.

ℓ = length of elastic portion of blade.

ℓ_e = length of finite element, nondimensionalized with respect to ℓ.

m = mass per unit length of the blade.

2M = total number of modes used in flap lag analysis.

$[M]$ = mass matrix, defined in Appendix B.

N = number of element shape functions (4).

P = differential operator.

q = unknown function.

q^g = global approximation to q.

q^e = element, (local) approximation to q.

$\underset{\sim}{q} = \begin{Bmatrix} \overline{v} \\ \overline{w} \end{Bmatrix}$ = vector of unknown lag and flap displacements.

R_e = blade elastic coupling parameter.

R = blade radius.

$R, \overline{R}$ = differential operators.

$\overline{r}_e = r_{e/\ell}$ = $\overline{x}_0$ coordinate of inboard node of element e.

$[S_B]$ = bending stiffness operator, defined in Appendix B.

$[S_{T1}]$ = centrifugal tension operator, defined in Appendix B.

$[S_L]$ = matrix of linear terms in the static equilibrium equations, Appendix B.

$[S_{NL}]$ = matrix of nonlinear terms in the static equilibrium position equations, Appendix B.

$\bar{T} = \frac{T}{m\Omega^2 \ell^2}$

t = time.

$[T_1], [T_2], [T_1^e], [T_2^e], [T_2^{ei}]$ = tension operators and matrices defined in Appendix B.

u = axial displacement of blade, inextensional.

$\bar{v}, \bar{v}^e$ = global and local lag displacement nondimensionalized with respect to ℓ.

$\bar{w}, \bar{w}^e$ = global and local flap displacement nondimensionalized with respect to ℓ.

$\bar{x}_0 = x_{0/\ell}$ = spanwise coordinate for elastic portion of the blade.

$\bar{x}_e = x_{c/\ell}$ = element coordinate.

β_1 = first fundamental frequency beam constant.

β_p = precone angle.

$\Gamma = \frac{\gamma \ell^4}{6R^4}$

$\gamma = \frac{2\rho_A b R^4}{1/3 m \ell^3}$ = Lock number

$\underset{\sim}{\gamma} = \{\gamma_n\}$ = vector of element lag interpolation polynomial

ε = residual

ζ_n^e = element shape function, defined in global domain.

$\underset{\sim}{\eta} = \{\eta_n\}$ = vector of element flap interpolation polynomials.

θ = collective pitch setting.

λ = inflow ratio.

ρ_A = density of air.

σ = blade solidity ratio.

ϕ_m = global shape function.

$[\phi_m], [\phi]$ = matrix of global shape function.

$[\bar{\Phi}]$ = modal transformation matrix.

$\bar{\omega}_{L1NR} = \frac{EI_2}{m\Omega^2 \ell^4}(\beta_1 \ell)^4$ = first nonrotating lag frequency.

$\bar{\omega}_{F1NR} = \frac{EI_3}{m\Omega^2 \ell^4}(\beta_1 \ell)^4$ = first nonrotating flap frequency.

$\bar{\omega}_{L1}, \bar{\omega}_{F1}$ = first rotating uncoupled lag and flap frequency, nondimensionalized with respect to Ω.

Ω = speed of rotation.

$\psi = \Omega t$ = azimuth angle, dimensionless time coordinate.

ψ_n^e = element shape functions.

$$[\psi] = \begin{bmatrix} \gamma^T & \underset{\sim}{0} \\ \underset{\sim}{0} & \underset{\sim}{\eta}^T \end{bmatrix}$$

Special Symbols

$(\dot{}) = \frac{1}{\Omega}\frac{d}{dt} = \frac{d}{d\psi}$

$(\ )_{,x} = \frac{\partial}{\partial \bar{x}_0}$

$(\ )^0$ = steady state portion of a quantity.

$\Delta(\ )$ = perturbation portion of a quantity.

$(\underset{\sim}{\ })$ = vector or matrix quantity.

$[\ ]^s$ = assembled system matrix.

Appendix B: Definition of Various Expressions

$$\bar{x}_0 = \bar{x}_e + \bar{r}_e$$

$$[A_1] = \Gamma \begin{bmatrix} -2\frac{R}{\ell}\lambda\beta_p + \theta\bar{x}_0\beta_p & 0 \\ \bar{x}_0\beta_p & 0 \end{bmatrix}$$

$$[A_2] = \Gamma \begin{bmatrix} (\theta\bar{x}_0 - 2\frac{R}{\ell}\lambda)\bar{w}_{,x} + \lambda\frac{R}{\ell}\bar{x}_0\bar{w}_{,x}D_x & 0 \\ \bar{x}_0\bar{w}_{,x} - \bar{x}_0^2\bar{w}_{,x}D_x & 0 \end{bmatrix}$$

$$[A_1^e] = \Gamma\int_0^{\ell_e}\begin{bmatrix} \underset{\sim}{\gamma}\underset{\sim}{\gamma}^T(-2\frac{R}{\ell}\lambda\beta_p + \theta\beta_p\bar{x}_0) & \underset{\sim}{0} \\ \underset{\sim}{\eta}\underset{\sim}{\gamma}^T x_0\beta_p & \underset{\sim}{0} \end{bmatrix} d\bar{x}_e$$

$$[A_2^3] = \Gamma\int_0^{\ell_e}\begin{bmatrix} \underset{\sim}{\gamma}\underset{\sim}{\gamma}^T(\theta\bar{x}_0 - 2\frac{R}{\ell}\lambda)\underset{\sim}{\eta}_{,x}^T g^{e0} + \underset{\sim}{\gamma}\underset{\sim}{\gamma}_{,x}\frac{R}{\ell}\bar{x}_0\underset{\sim}{\eta}_{,x}^T g^{e0} & \underset{\sim}{0} \\ \underset{\sim}{\eta}\underset{\sim}{\gamma}^T\bar{x}_0\underset{\sim}{\eta}_{,x}^T g^{e0} - \underset{\sim}{\eta}\underset{\sim}{\gamma}_{,x}\bar{x}_0^2\underset{\sim}{\eta}_{,x}^T g^{eo} & \underset{\sim}{0} \end{bmatrix} d\bar{x}_e$$

$$[A_2^e] = \Gamma\int_0^{\ell_e}\left[\begin{array}{c:c} \underset{\sim}{\gamma}\underset{\sim}{\gamma}^T(\theta\bar{x}_0 - 2\frac{R}{\ell}\lambda)\underset{\sim}{\eta}_{,x}^T g^{e0} + \underset{\sim}{\gamma}\underset{\sim}{\gamma}_{,x}^T\frac{R}{\ell}\lambda\bar{x}_0\underset{\sim}{\eta}_{,x}^T g^{e0} & \underset{\sim}{\gamma}\underset{\sim}{\eta}_{,x}^T(\theta\bar{x}_0 - 2\frac{R}{\ell})\underset{\sim}{\gamma}^T h^{e0} + \underset{\sim}{\gamma}\underset{\sim}{\eta}_{,x}^T\frac{R}{\ell}\bar{x}_0\lambda\underset{\sim}{\eta}_{,x}^T h^{e0} \\ \underset{\sim}{\eta}\underset{\sim}{\gamma}_{,x}^T\bar{x}_0\underset{\sim}{\eta}_{,x}^T g^{e0} - \underset{\sim}{\eta}\underset{\sim}{\gamma}_{,x}^T\bar{x}_0^2\underset{\sim}{\eta}_{,x}^T g^{e0} & \underset{\sim}{\eta}\underset{\sim}{\eta}_{,x}^T(\bar{x}_0\underset{\sim}{\gamma}^T h^{e0} - \bar{x}_0^2\underset{\sim}{\gamma}_{,x}^T h^{e0}) \end{array}\right] d\bar{x}_e$$

$$[B] = \begin{bmatrix} B_{22} & B_{23} \\ B_{23} & B_{33} \end{bmatrix}$$

$$[B^e] = \int_0^{\ell_e}\begin{bmatrix} \underset{\sim}{\gamma}_{,x}\underset{\sim}{\gamma}_{,x}^T B_{22} & \underset{\sim}{\gamma}_{,x}\underset{\sim}{\eta}_{,x}^T B_{23} \\ \underset{\sim}{\eta}_{,x}\underset{\sim}{\gamma}_{,x}^T B_{23} & \underset{\sim}{\eta}_{,x}\underset{\sim}{\eta}_{,x}^T B_{33} \end{bmatrix} d\bar{x}_e$$

$$[C_{Ax}] = \begin{bmatrix} 2\int_0^{\bar{x}_0}(\bar{v}_{,x}D_x) & 2\int_0^{\bar{x}_0}(\bar{w}_{,x}D_x) \\ 0 & 0 \end{bmatrix} d\bar{x}_0$$

$$[C_{Ax}^e] = \int_0^{\ell_e}\left[\gamma 2(\underset{\sim}{h}^{e0})^T\int_0^{\bar{x}_e}\underset{\sim}{\gamma}_{,x}\underset{\sim}{\gamma}_{,x}^T d\bar{x}_e \;\vdots\; \gamma 2(g^{e0})^T\int_0^{x_e}\underset{\sim}{\eta}_{,x}\underset{\sim}{\eta}_{,x}^T d\bar{x}_e\right] d\bar{x}_e$$

$$[C_{Ax}^{ei}] = \left[\begin{array}{c:c} \int_0^{\ell_e} d\bar{x}_e 2(h^{io})^T\int_0^{\ell_i}\underset{\sim}{\gamma}_{,x}\underset{\sim}{\gamma}_{,x}^T d\bar{x}_i & \int_0^{\ell_e} d\bar{x}_e 2(g^{io})^T\int_0^{\ell_i}\underset{\sim}{\eta}_{,x}\underset{\sim}{\gamma}_{,x}^T d\bar{x}_i \\ \underset{\sim}{0} & \underset{\sim}{0} \end{array}\right]$$

$$[C_{T2}] = \begin{bmatrix} 2D_x(\bar{v}_{,x}\int_{x_0}^{1}) & 0 \\ 2D_x(\bar{w}_{,x}\int_{x_0}^{1}) & 0 \end{bmatrix}$$

$$\{C\} = [\bar{\Phi}]^T\{F^s\}$$

$$[D_1] = \Gamma\begin{bmatrix} \theta\frac{R}{\ell}\lambda + 2\frac{C_{do}}{a}\bar{x}_0 & \theta(\bar{x}_0 + \bar{e}_1) - 2\frac{R}{\ell}\lambda \\ \frac{R}{\ell}\lambda - 2\theta\bar{x}_0 & \bar{x}_0 + \bar{e}_1 \end{bmatrix}$$

$$[D_2] = \Gamma\begin{bmatrix} \theta\dot{\bar{w}} & -2\beta_p\bar{v} - \dot{\bar{w}} \\ 0 & \dot{\bar{v}} \end{bmatrix}$$

$$[D_3] = \Gamma\begin{bmatrix} 0 & -\bar{v}\bar{w}_{,x^2} + \bar{x}_0\bar{v}_{,x}\bar{w}_{,x} \\ 0 & 0 \end{bmatrix}$$

$$[D_1^e] = \int_0^{\ell_e} ([\Psi]^T[D_1][\Psi])d\bar{x}_e$$

$$[D_2^e] = \Gamma\int_0^{\ell_e}\begin{bmatrix} \underset{\sim}{0} & \underset{\sim}{\gamma}\underset{\sim}{\eta}^T 2\beta_p\underset{\sim}{\gamma}^T\underset{\sim}{h}^{e0} \\ \underset{\sim}{0} & \underset{\sim}{0} \end{bmatrix}d\bar{x}_e$$

$$[D_3^e] = \Gamma\int_0^{\ell_e}\begin{bmatrix} \underset{\sim}{0} & (\underset{\sim}{g}^{0e})^T\underset{\sim}{\eta}_{,x}\underset{\sim}{\gamma}\underset{\sim}{\eta}^T(\bar{x}_0\underset{\sim}{\gamma}^T_{,x}\underset{\sim}{h}^{e0} - 2\underset{\sim}{\gamma}^T\underset{\sim}{h}^{e0} \\ \underset{\sim}{0} & \underset{\sim}{0} \end{bmatrix}d\bar{x}_e$$

$$[D] = [\bar{\Phi}]^T([G]^S + [D_1]^S - [D_2]^S + [D_3]^S + [T_2]^S + [T_2]^{Si} - [C_{Ax}]^S - [C_{Ax}]^{Si})[\bar{\Phi}]$$

$$\{F\} = -\begin{Bmatrix} 0 \\ \beta_p(\bar{x}_0 + \bar{e}_1) \end{Bmatrix} + \Gamma\begin{Bmatrix} -\theta(\bar{x}_0 + \bar{e}_1)\frac{R}{\ell}\lambda + (\frac{R}{\ell})^2\lambda^2 - \frac{Cd_o}{a}\bar{x}_0(\bar{x}_0 + 2\bar{e}_1) \\ \theta\bar{x}_0(\bar{x}_0 + 2\bar{e}_1) - (\bar{x}_0 + \bar{e}_1)\frac{R}{\ell}\lambda \end{Bmatrix}$$

$$\{F^e\} = \int_0^{\ell_e}[\Psi]^T\{F\}d\bar{x}_e \; ; \quad [G] = \begin{bmatrix} 0 & -2\beta_p \\ 2\beta_p & 0 \end{bmatrix}$$

$$[I] = \begin{bmatrix} 1 & 0 \\ 0 & 1 \end{bmatrix} \; ; \quad [G^e]\int_0^{\ell_e}([\Psi]^T[G][\Psi])d\bar{x}_e$$

$$[I^e] = \int_0^{\ell_e}([\Psi]^T[I][\psi])d\bar{x}_e \; ; \qquad [K_{ROT}] = \begin{bmatrix} 1 & 0 \\ 0 & 1 \end{bmatrix}$$

$$[K_{ROT}^e] = \int_0^{\ell_e}([\Psi]^T[K_{ROT}][\Psi])d\bar{x}_e$$

$$[K] = [\bar{\Phi}]^T([B]^S + [T_1]^S - [K_{ROT}]^S + [A_1]^S + [\bar{A}_2]^S)[\bar{\Phi}]$$

$$[M] = [\bar{\Phi}]^T[I]^S[\bar{\Phi}]$$

$$[S_B] = \begin{bmatrix} B_{22}D_x^4 & B_{23}D_x^4 \\ B_{23}D_x^4 & B_{33}D_x^4 \end{bmatrix}$$

$$[S_{T1}] = \begin{bmatrix} D_x(T_1D_x) & 0 \\ 0 & D_x(T_1D_x) \end{bmatrix}$$

$$T_1 = \tfrac{1}{2}[(1 + 2e_1) - \bar{x}_0(\bar{x}_0 + 2e_1)]$$

$$[S_L] = [\bar{\Phi}]^T([B]^S + [T_1]^S - [K_{ROT}]^S + [A_1]^S)[\bar{\Phi}]$$

$$[S_{NL}] = [\bar{\Phi}]^T[A_2]^S[\bar{\Phi}]$$

$$[T_1] = \begin{bmatrix} T_1D_x & 0 \\ 0 & T_1D_x \end{bmatrix}$$

$$T_2 = \begin{bmatrix} 2\bar{v}_{,x} \int_{\bar{x}_0}^{1} (\,) & 0 \\ 2\bar{w}_{,x} \int_{\bar{x}_0}^{1} (\,) & 0 \end{bmatrix}$$

$$\underset{\sim}{\gamma} = \underset{\sim}{\eta} = \begin{bmatrix} 1 - 3\dfrac{\bar{x}_e^2}{\ell_e^2} + 2\dfrac{\bar{x}_e^2}{\ell_e^2} \\ \bar{x}_e\left(1 - 2\dfrac{\bar{x}_e}{\ell_e} + \dfrac{\bar{x}_e^2}{\ell_e^2}\right) \\ 3\dfrac{\bar{x}_e^2}{\ell_e^2} - 2\dfrac{\bar{x}_e^3}{\ell_e^3} \\ \bar{x}_e\left(-\dfrac{\bar{x}_e}{\ell_e} + \dfrac{\bar{x}_e^2}{\ell_e^2}\right) \end{bmatrix}$$

$$[T_1^e] = \int_0^{\ell_e} \begin{bmatrix} \underset{\sim}{\gamma}_{,x}\underset{\sim}{\gamma}_{,x}^T T_1 & 0 \\ 0 & \underset{\sim}{\eta}_{,x}\underset{\sim}{\eta}_{,x}^T T_1 \end{bmatrix} d\bar{x}_e$$

$$[T_2^e] = \int_0^{\ell_e} \begin{bmatrix} \underset{\sim}{\gamma}_{,x}\underset{\sim}{\gamma}_{,x}^T \underset{\sim}{h}^{e0}{}_2 \int_{\bar{x}_e}^{\ell_e} \underset{\sim}{\gamma}^T d\bar{x}_e & \underset{\sim}{0} \\ \underset{\sim}{\eta}_{,x}\underset{\sim}{\eta}_{,x}^T \underset{\sim}{g}^{e0}{}_2 \int_{\bar{x}_e}^{\ell_e} \underset{\sim}{\gamma}^T d\bar{x}_e & \underset{\sim}{0} \end{bmatrix} d\bar{x}_e$$

$$[T_2^{ei}] = \begin{bmatrix} \int_0^{\ell_e} \underset{\sim}{\gamma}_{,x}\underset{\sim}{\gamma}_{,x}^T d\bar{x}_e \underset{\sim}{h}^{e0}{}_2 \int_0^{\ell_i} \underset{\sim}{\gamma}^T d\bar{x}_i & \underset{\sim}{0} \\ \int_0^{\ell_e} \underset{\sim}{\eta}_{,x}\underset{\sim}{\eta}_{,x}^T d\bar{x}_e \underset{\sim}{g}^{e0}{}_2 \int_0^{\ell_i} \underset{\sim}{\gamma}^T d\bar{x}_i & \underset{\sim}{0} \end{bmatrix}$$

TABLE 1: COMPARISON OF GLOBAL GALERKIN AND FINITE ELEMENT GALERKIN METHODS

$\sigma = 0.05$; $\bar{e}_1 = 0$; $\gamma = 5.0$; $\bar{\omega}_{F1NR} = 0.4$; $\omega_{L1NR} = 1.1$; $R_e = 1.0$

Finite element results based on 3 elements and 1 mode per degree of freedom
Global Galerkin results based on 1 mode per degree of freedom.

	Global Galerkin $\theta = 0.20$	FEM $\theta = 0.20$	Global Galerkin $\theta = 0.45$	FEM $\theta = 0.45$
$\bar{\omega}_{L1}(\theta=0)$	1.179967	1.18026	1.179967	1.18026
$\bar{\omega}_{F1}(\theta=0)$	1.140290	1.14150	1.140290	1.14150
h^0	.016719	.016484 (-1.4%)	.087953	.086768 (-1.3%)
g^0	.070289	.066521 (-5.4%)	.187816	.177959 (-5.2%)
ζ_1 lag	-.026198	-.026168 (-.11%)	-.066079	-.065838 (-.36%)
ζ_1 flap	-.307892	-.308048 (.05%)	-.28126	-.281628 (.13%)

$$\Delta\% = \frac{\text{FEM-Global Galerkin}}{\text{Global Galerkin}}$$

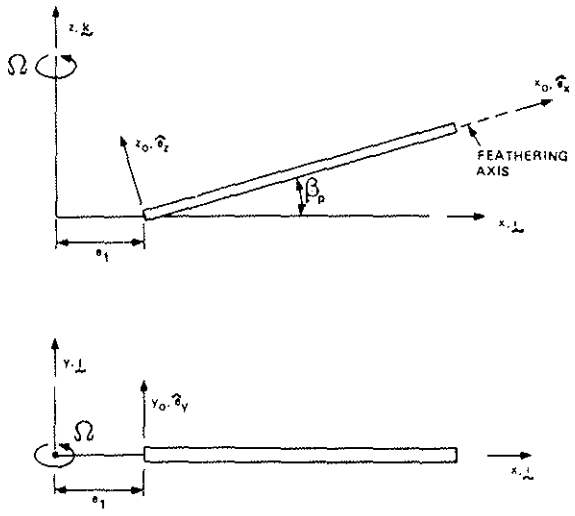

Figure 1a. Typical Description of the Undeformed Blade in the Rotating System x,y,z ($\underset{\sim}{i},\underset{\sim}{j},\underset{\sim}{k}$)

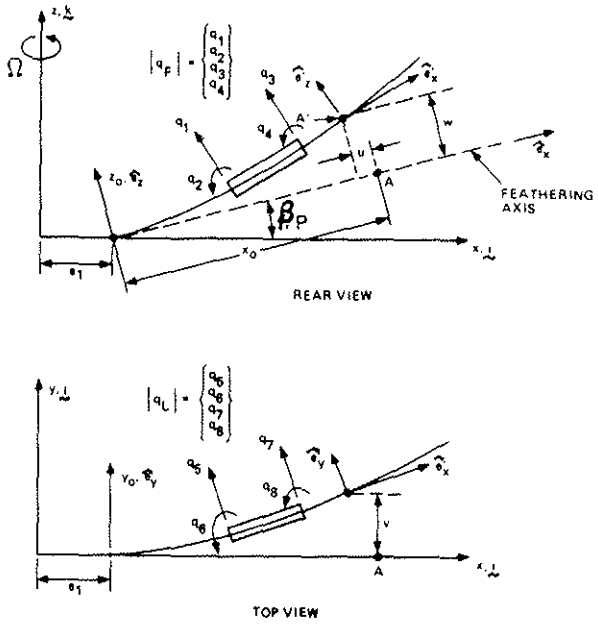

Figure 1b. Geometry of the Elastic Axis of the Deformed Blade and Schematic Description of the Finite Element Model

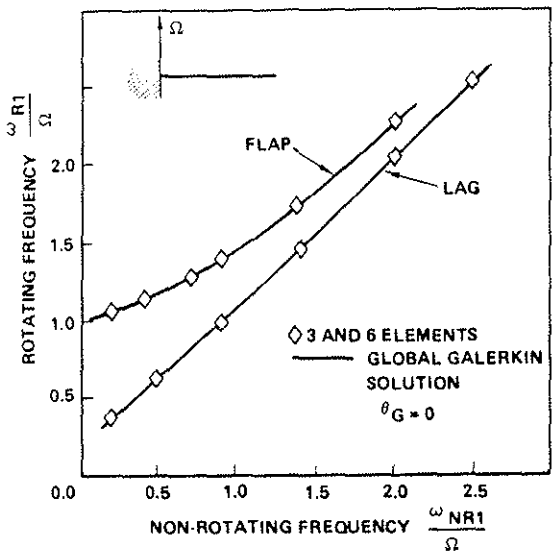

Figure 2. Comparison of the Methods in Calculating Fundamental Flap and Lag Frequencies of a Rotating Blade

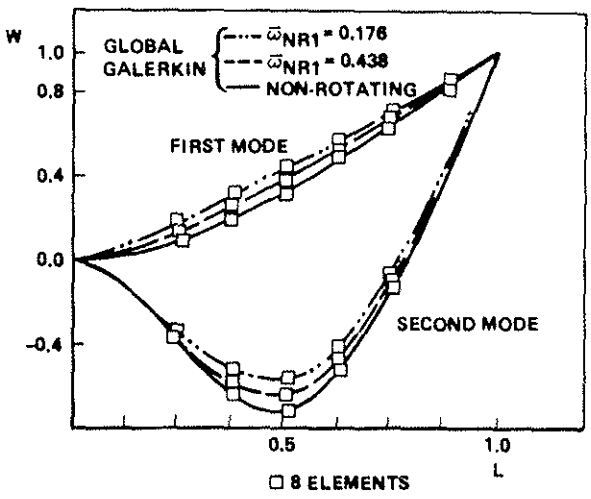

Figure 3. Comparison of the Methods in Calculating First and Second Flapwise Mode Shapes of a Rotating Beam

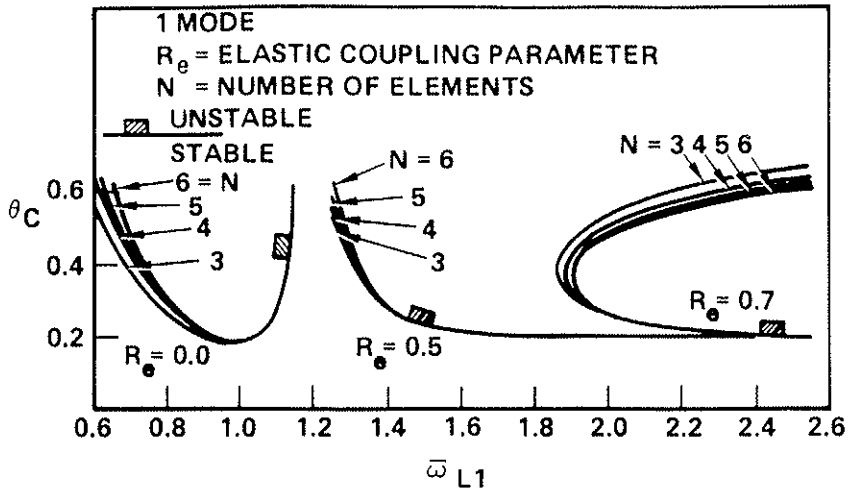

Figure 4. Convergence of the Flap-Lag Stability Boundaries when the Number of Elements is Changed* (σ = 0.05; γ = 5.0; $\bar{e}_1$ = 0; $\bar{\omega}_{F1}$ = 1.0689)

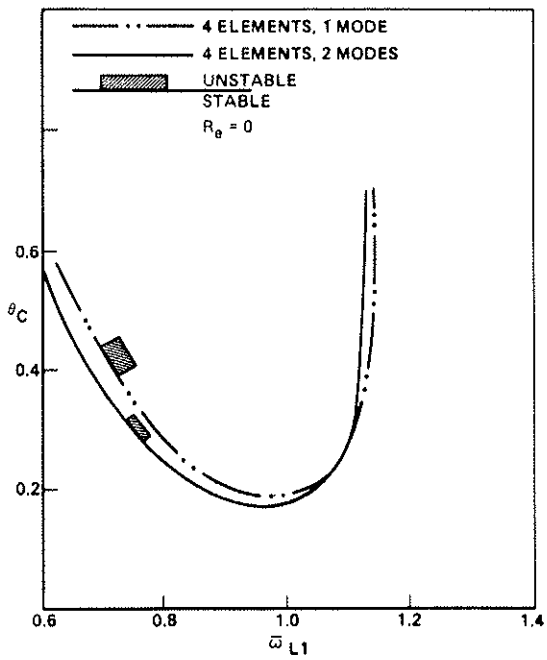

Figure 5. Convergence of Flap-Lap Stability Boundaries when the Number of Modes is Changed* (σ = 0.05; γ = 5.0; $\bar{e}_1$ = 0; $\bar{\omega}_{F1}$ = 1.0689)

*θ_C = is critical collective pitch setting at which linearized system becomes unstable